INTERNATIONAL JOURNAL
FOR INNOVATION
EDUCATION AND RESEARCH
ISSN: 2411-2933

Journal URL: https://scholarsjournal.net/index.php/ijier

Project and analysis of a dual band CPW-fed antenna for WBAN applications

Angélica Quadros, Federal University of Pará
Miércio Neto, Federal University of Pará

Abstract

A compact and low profile wearable antenna project is presented for WBAN (wireless body area network) applications. The proposed patch antenna has an experimental geometry and is designed using the semi flexible substrate Rogers 5880, very common in wearable devices. It is CPW-fed and operates in two main frequencies: 3.5 GHz (WiMAX wireless communication standard) and 5.8 GHz (Industrial, Scientific, and Medical band). Using CST Studio to design and simulate, the main antenna parameters such as coefficient reflexion, impedance, gain and current distribution were analyzed to understand the behavior of the antenna. The results showed a reasonably satisfactory performance, suggesting some changes to improve the impedance and indicating a huge potential for medical devices.

Keywords: dual-band antenna; WBAN; CPW; 5.8 GHz; 3.5 GHz.

1. Introduction

In this century, the world has been watching a growth in the research and development of flexible and wearable devices and sensors which can monitor and transmit vital signals in various body-worn applications. Some devices became more popular, for example portable health care and sports monitoring devices. Other ones can even be considered as essentials for health monitoring and geopositioning of rescue or military personals etc. This context has led to the foundation of wireless body area network (WBAN) [1], which is among the most attractive applications [2].

The antenna plays a crucial role in ensuring the operation of a WBAN system [2] and to maintain a consistent performance [3]. As the antenna of a WBAN can be placed on a human body, the influence of the wearer on the transient characteristics should be considered in the antenna design [2]. Convenience, durability, acceptable gain, high efficiency, low Specific Absorption Rate (SAR) have become important characteristics of the wearable antenna [4]. At the same time, they have to be compact, low profile, mechanically robust and lightweight [5]. A lot of researches in WBAN presented antennas designed for operation in 2.45 GHz band, but the 5.8 GHz band seems to be one of the preferred choices [3].

The user's data can be transmitted by two forms: the on-body and off-body communications. In the first one, the wearable devices communicate closely distant from the human body. The off-body communication transmits the data to remote devices for analysis by physicians and experts [6]. Several off-body communication antennas, with and without the integration of flexible/textile materials, have been proposed for wearable applications in the 2.4/5.8 GHz industrial, scientific, and medical (ISM) bands [7].

A flexible substrate is suitable for wearable implementations as they need to provide flexibility of usage and a comfortable user experience [8]. Relevant works used Rogers 5880 as substrate in WBAN applications antennas with different kinds of design. Targeting the on-body communication wearable devices, the multiband antenna proposed in [8] used Rogers 5880, and covers the 2.4 GHz/5.2 GHz/5.8 GHz WLAN,

3.5 GHz WiMAX, and 4.4 GHz C-bands. In [9], the same substrate was chosen to simulate a fractal antenna for WBAN applications. The authors in [10] performed a comparison between the very common substrate FR-4 and Rogers 5880 in a head-worn antenna at 5.8 GHz, concluding that Rogers 5880 provided a lower SAR and a higher gain. Recently, the authors in [7] have chosen Rogers 5880 as substrate to construct a flexible circular polarized wearable antenna for WBAN communications operating at 5.8Ghz.

The antenna developed in [11] has two main resonances, where the first one is at 3.5 GHz, which can serve the WiMAX communication standard, while the second is at 5.8 GHz, which can serve the ISM-band. Similarly, the wearable antenna presented in [12] resonates at 3.5GHz, for data transmission over WiMAX wireless communication standard, and 5.8 GHz, targeting the medical application.

Another important feature is the antenna feed. Numerous articles have decided to use coplanar waveguide (CPW) in WBAN projects, such as [4], [6], [7] and [8]. In 2019 the dual band antenna for medical applications proposed in [13] obtained omnidirectional radiation patterns by feeding with CPW. The multiband microstrip antenna designed in [14] for wireless communication application, which includes WBAN, was also fed by CPW.

This work proposes a compact low profile dual-band antenna with operation at 3.5 GHz, for data transmission over WiMAX wireless communication standard, and 5.8 GHz of the ISM Band, which can easily fit any wearable and conformal wireless device [7], for targeting the WBAN application.

2. Antenna design

The antenna was designed and simulated using CST Microwave Studio 2020 software [15], which is based on FIT (Finite Integration Technique) [10]. The proposed antenna is composed of a ground plane below, followed by the substrate and, above, the radiating element. The single layer semi-flexible Rogers Duroid 5880 substrate, with thickness=1.6 mm, has dielectric constant of 2.2 and tangent loss of 0.0009.

The antenna is fed with a 50 Ω CPW to provide good impedance. The patch antenna geometry consists of an "x" shape with circles at the ends, a curve in the center and a feed line, as shown in Fig. 1a. The radiating element and the feed line are PEC (Perfect Electric Conductor) 0.035 mm thick. The dimensions are described in Fig. 2b and the values in Table 1.

Figure 1. a) Antenna structure, b) Antenna dimensions.

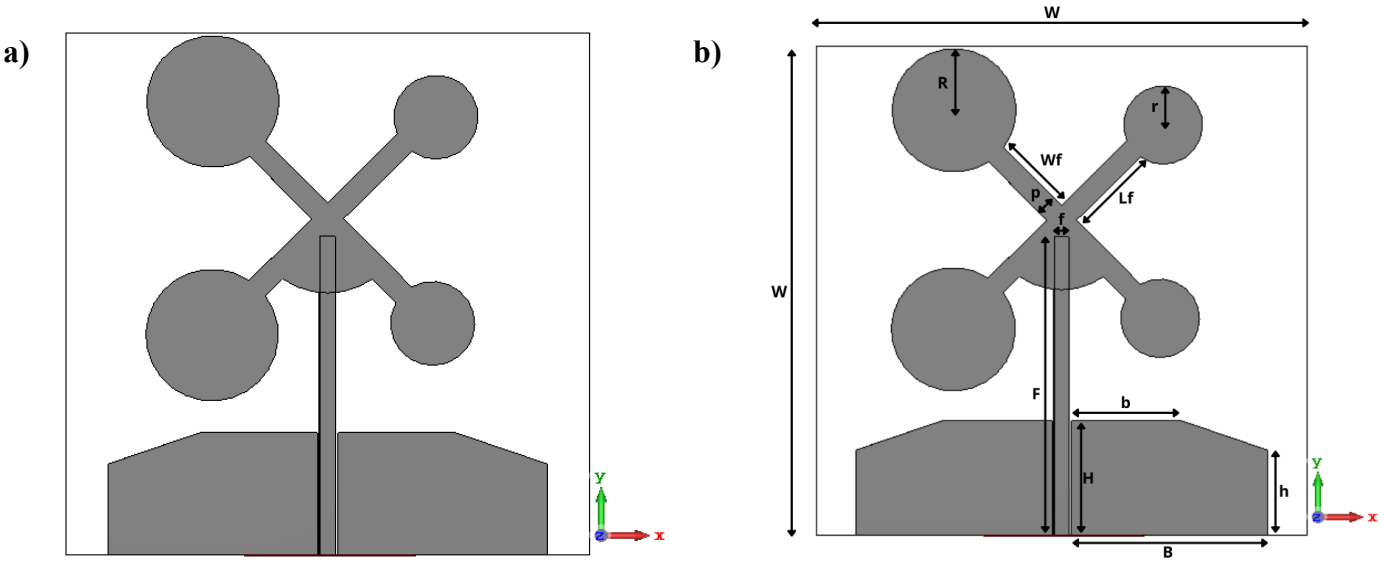

Table 1. Values of the antenna dimensions.

Parâmetros	Valores(mm)	Parâmetros	Valores (mm)
W	70	p	3.43
Wf	11.71	L f	13.13
R	8.84	r	5.63
B	27.99	b	5.74
H	16.33	h	12.13
F	42.77	f	2.20

To achieve the desired results, structural changes in the initial shape of the antenna were made throughout the development of the antenna. Some shapes were being modified and introduced, as well as the width and length of the patch were also modified according to the responses seen in the simulations, aiming the low profile characteristic. These changes were essential to achieve the desired resonant frequencies of 3.5 GHZ and 5.8 GHZ.

3. Results and discussion

As mentioned above, all simulations were carried out with CST Studio, in the frequency range of 3 GHz to 6.5GHz, therefore all analyzes were made based on the results of the referred software. To carry out the simulation, it is necessary to excite the antenna, and for that, a CST Studio tool called Waveguide port is used. Another aspect to be considered before simulating is to set the operating frequency, which in this case are two (3.5 GHz and 5.8 GHz) to define virtual test points in the Field Monitors tool, allowing to obtain the representation of the radiation diagram in planes E and H. Fig. 2 shows the simulation environment and the excitation port.

Figure 2. CST Studio environment with the excitation port in red.

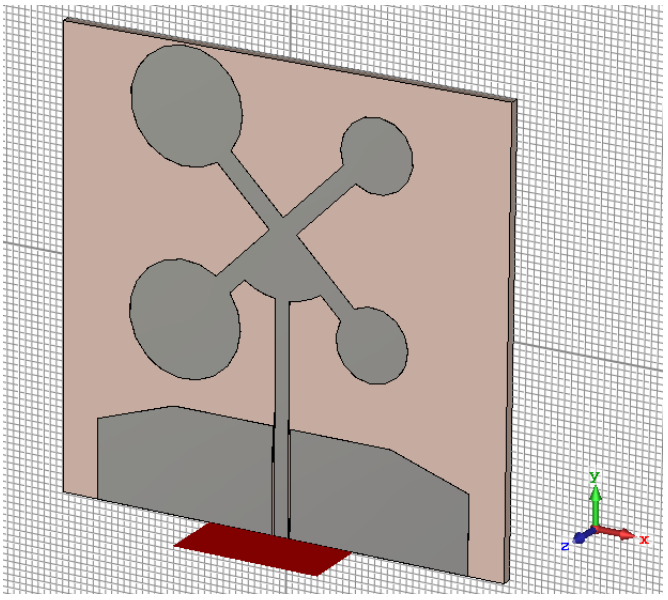

3.1 Return loss

The return loss indicates the ratio of incident power to reflected power [16]. In many works, the authors use

the -10 dB level as the threshold for defining the bandwidth, where this level represents 90% of the transmitted power and 10% of the reflected power. Fig. 3 shows that the antenna resonates over two frequency bands with operating frequencies 3.5 GHz and 5.8 GHz with return loss values −12.547, −11.125, respectively.

Figure 3. Simulated return loss performance.

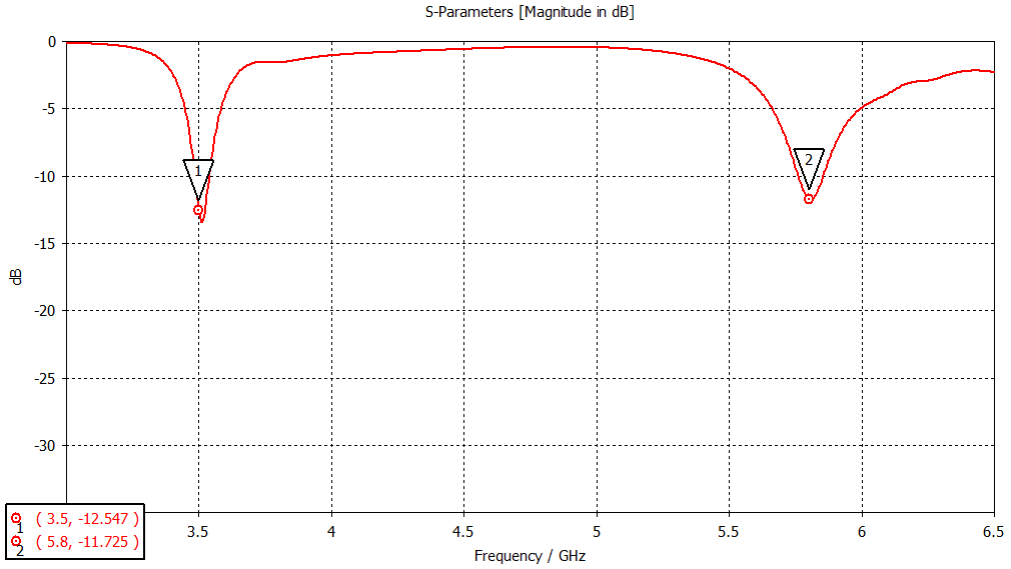

3.2 Efficiency

Efficiency is measured by the ratio between radiated power and input power. It indicates how much power is transmitted, given the power received. The total efficiency of an antenna takes into account the losses at the input terminals and inside the antenna structure, such as reflection losses due to the impedance mismatch between the transmission line and antenna and electrical losses due to conductors and dielectrics [16].

Fig. 4 shows both radiation e total efficiencies. The graph indicates a total efficiency of over 91% at both target frequencies. The radiation frequency shows even higher values, with efficiency of more than 96% at 3.5Ghz and more than 98% at 5.8GHz.

Figure 4. Radiation efficiency and total efficiency.

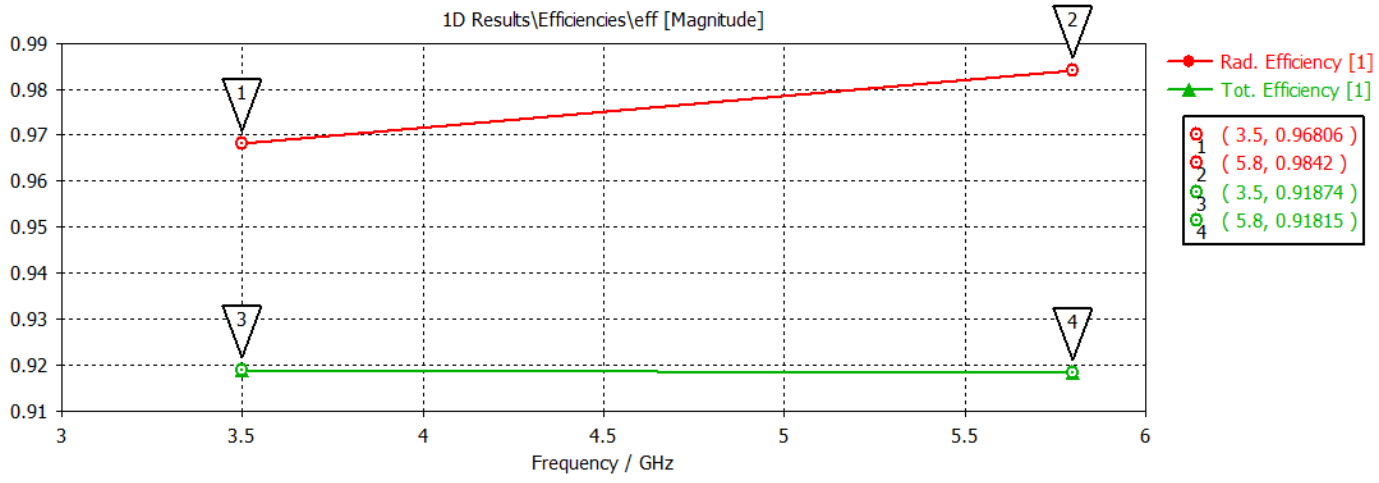

3.3 Impedance

The input impedance of an antenna is defined as the impedance presented by an antenna at its terminals or the ratio of voltage to current at the pair of terminals or the ratio of the appropriate components of the electric and magnetic fields at a point [17]. As shown in Fig. 5, the real part is near 50 Ω in both target frequencies, indicating a reasonably good impedance matching. An ideal antenna must not present an imaginary part, so the imaginary part must be as close to 0 as possible. The imaginary part in 3.5 GHz is closer to 0 than in 5.8 GHz (Fig. 6), although they are reasonably good values, it can be an indication of wasted energy, especially in 5.8 GHz.

Figure 5. Real impedance.

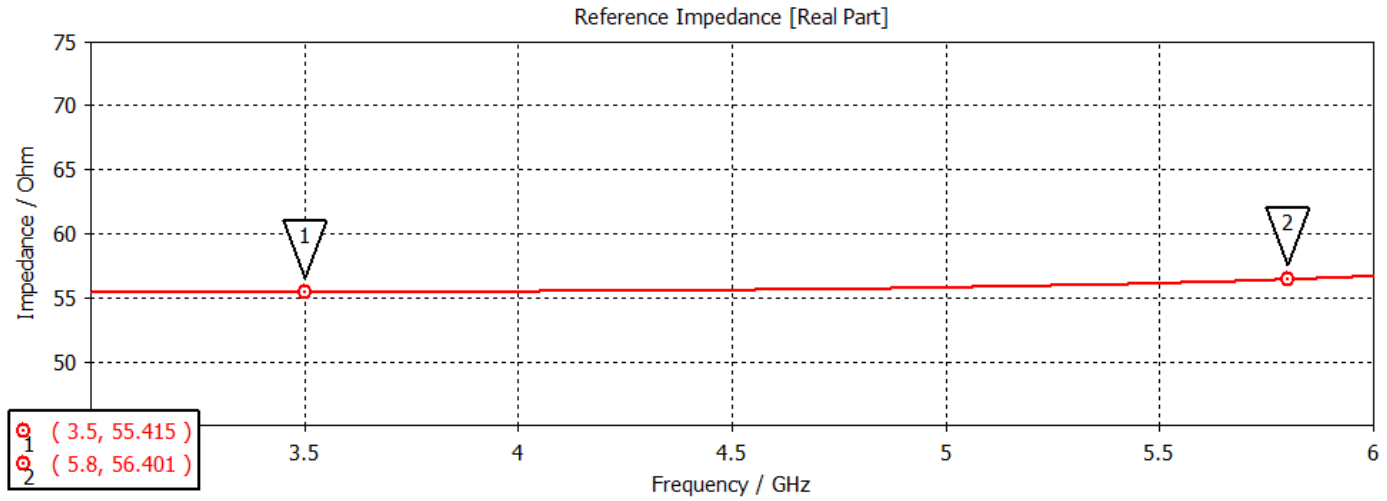

Figure 6. Imaginary impedance.

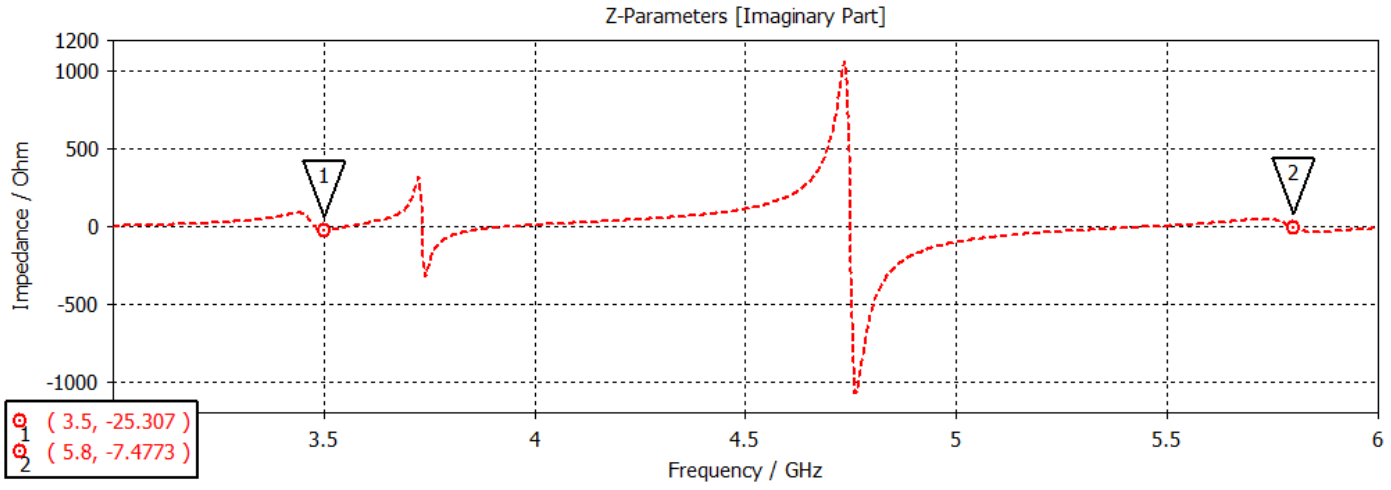

3.4 Gain

The gain is defined as the ratio between the radiation intensity in a given direction and the radiation intensity for an isotropic antenna. It takes into account both the efficiency and the directional properties of the antenna [18].

Fig. 7 presents the simulated gain performance of the proposed antenna. It is observed that the antenna gain

for proposed structure is less on low frequencies and comparatively more at high frequencies as given in Figure 7. Looking only to the target frequencies, the maximum gain achieved is 6.6 at 5.8 GHz. At 3.5 GHz, the gain is 4.7.

Figure 7. Gain.

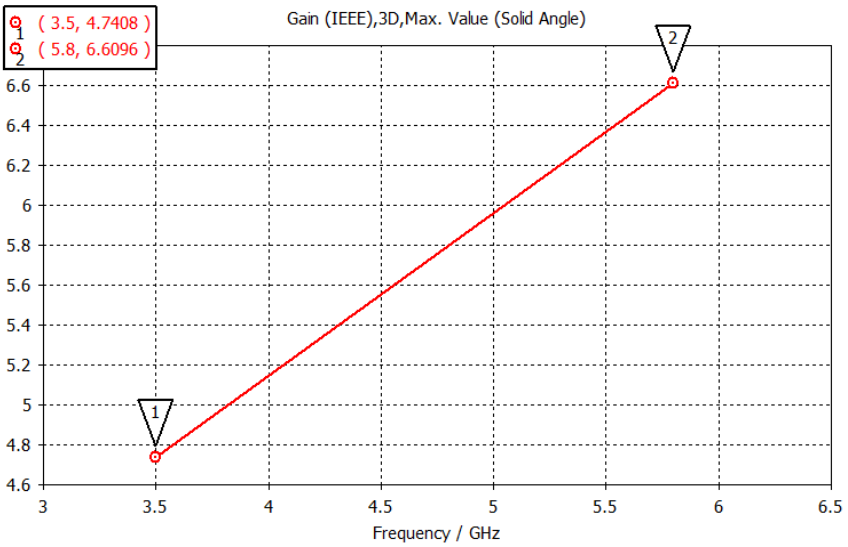

3.5 Radiation diagram

The simulated radiation patterns of the proposed dual band antenna are illustrated in Fig. 8. Different graphs are presented for different cuts, according to Phi= 0° (Fig. 8a), Phi= 90° (Fig. 8d), Theta= 0° (Fig. 8c) and Theta= 90° (Fig. 8d) cuts, at the resonant frequency 3.5 GHz. Observing Fig. 8a and Fig. 8b, the simulated results demonstrate that the proposed antenna has a directional radiation pattern at this frequency and there were no relevant variations in both Phi angles.

Figure 8. Radiation diagrams at 3.5 GHz.

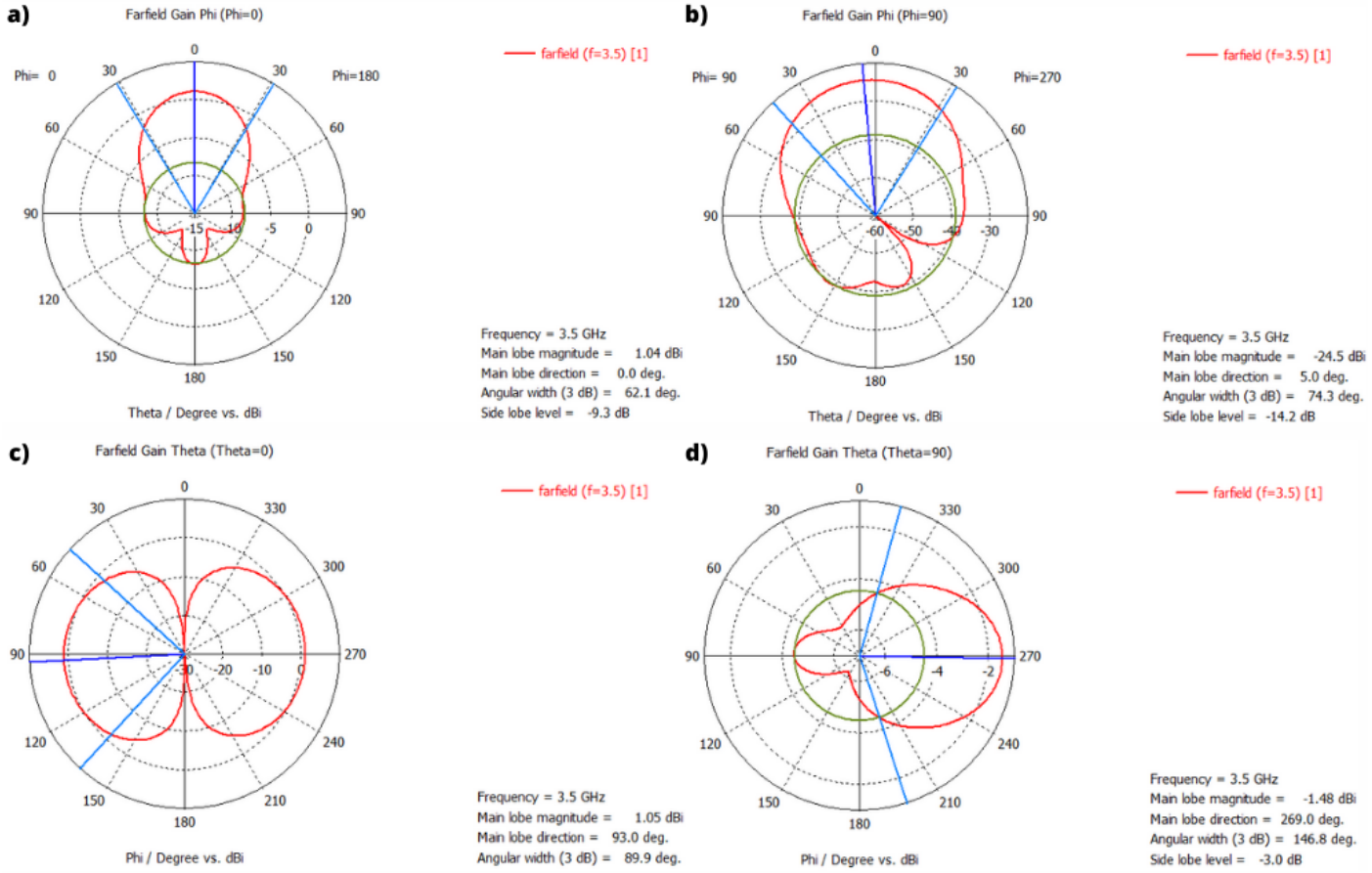

For the resonant frequency 5.8 GHz, the simulated radiation patterns are illustrated in Fig. 9. Different graphs are presented for different cuts, according to Phi= 0° (Fig. 9a), Phi= 90° (Fig. 9d), Theta= 0° (Fig. 9c) and Theta= 90° (Fig. 9d) cuts. Some null values were observed in Fig. 9a and Fig. 9b, which can be an because of the higher frequency in comparison with 3.5 GHz.

Figure 9. Radiation diagrams at 5.8 GHz.

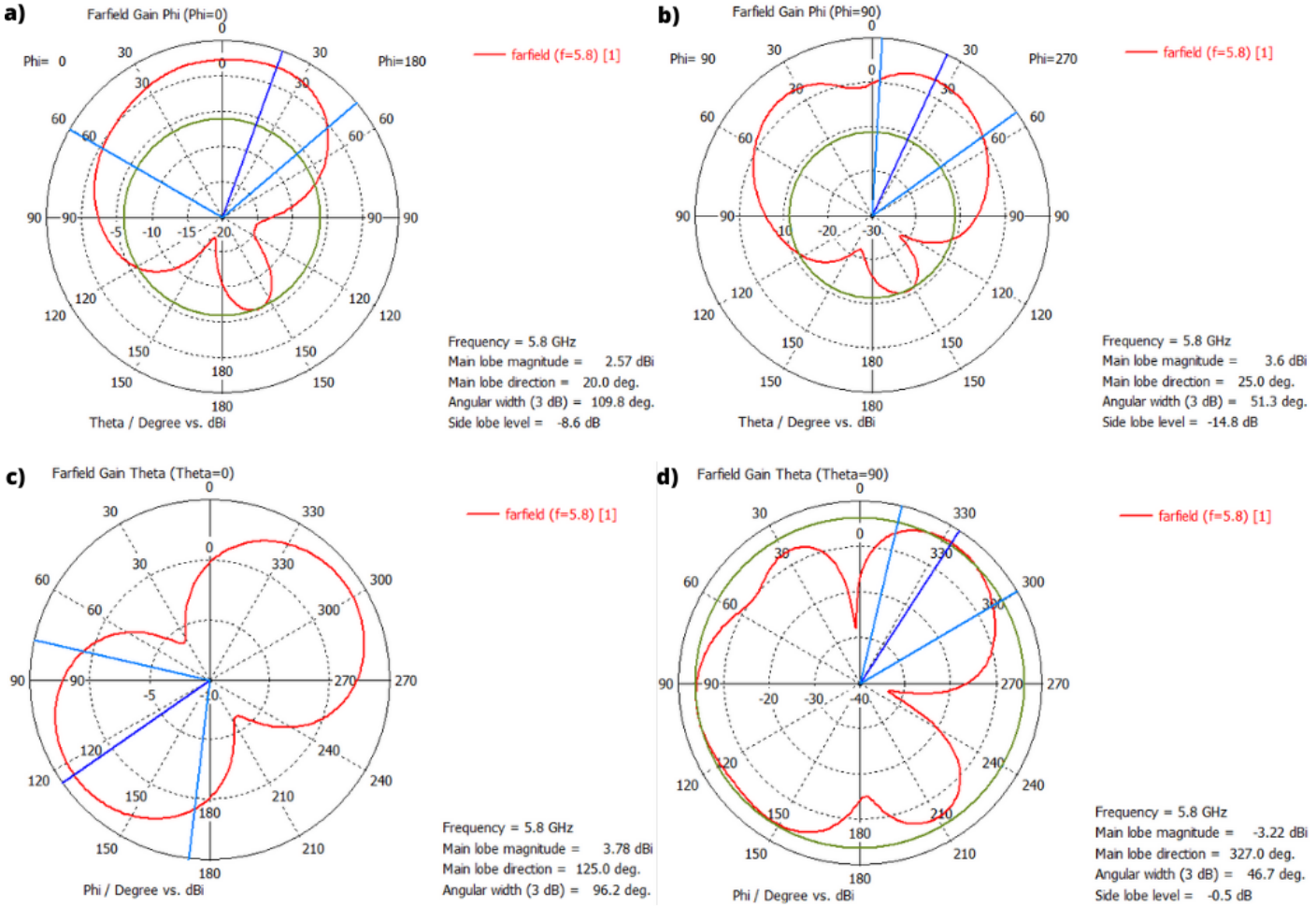

3.6 Electric field

As can be seen in Fig. 10, there is a greater concentration of current in the center line, on the sides of the lower structures and on the edges of the circles.

Figure 10. Electric field at 3.5 GHz.

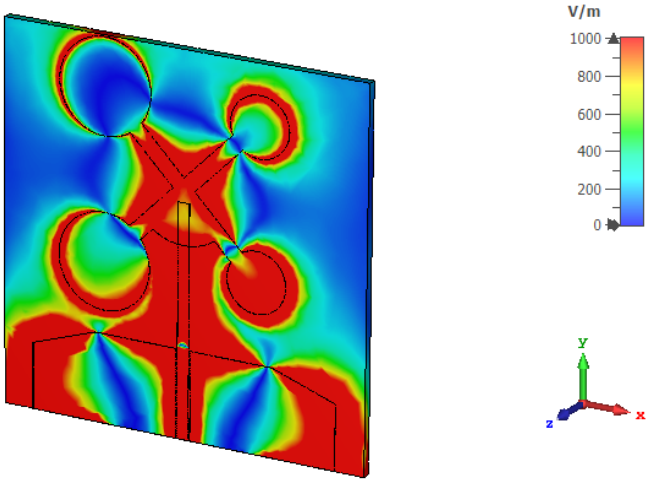

Observing the electric field graph in Fig. 12, there is a more intense electric field in the transmission line and patch compared to the distribution at the 3.5 GHz frequency.

Figure 11. Electric field at 5.8 GHz.

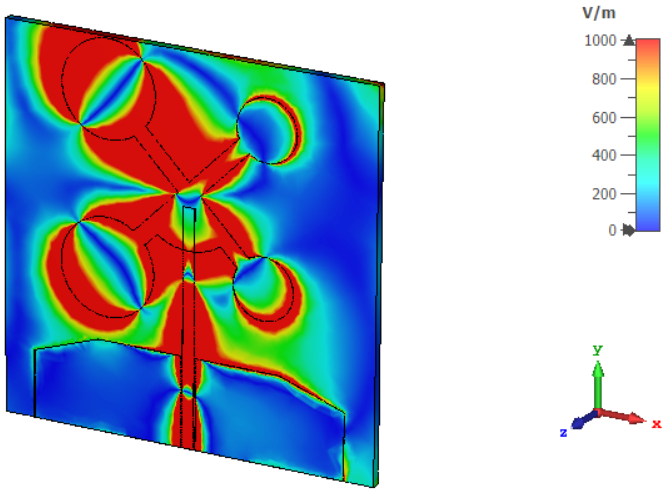

3.7 Current distribution

The simulated surface current distribution of the proposed antenna at the 3.5 GHz are presented in Fig. 12, to provide an overall view of the current repartition over the proposed antenna. Fig. 12 shows the bad distribution of the current at the ends of the antenna and its concentration in the lower structures and in the transmission line. This can be a consequence of mismatched impedance, as seen in the imaginary impedance (Fig. 6).

Figure 12. Current distribution at 3.5 GHz.

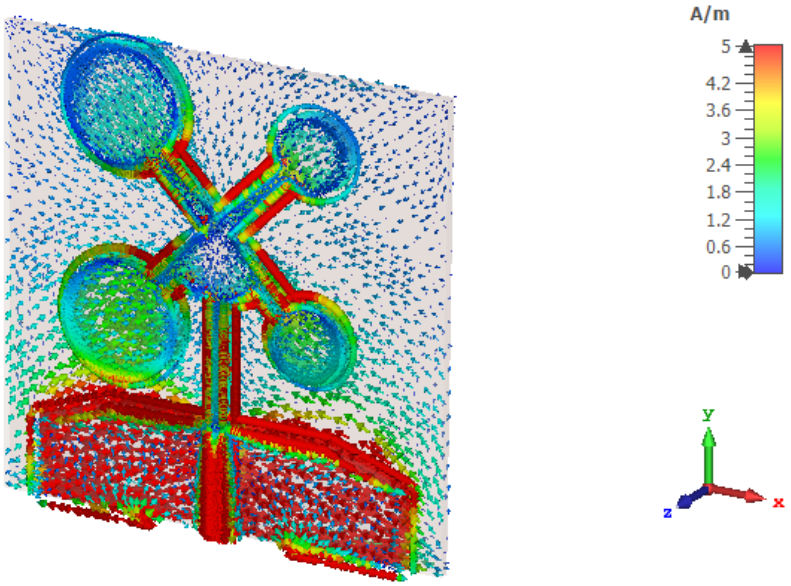

As already identified by the electric field analysis, the current distribution graph at the 5.8 GHz frequency

(Fig. 13) shows a higher concentration of current in the transmission line. The current is better distributed in the patch antenna than at 3.5 GHz, another consequence of the different imaginary impedance values at target frequencies.

Figure 13. Current distribution at 5.8 GHz.

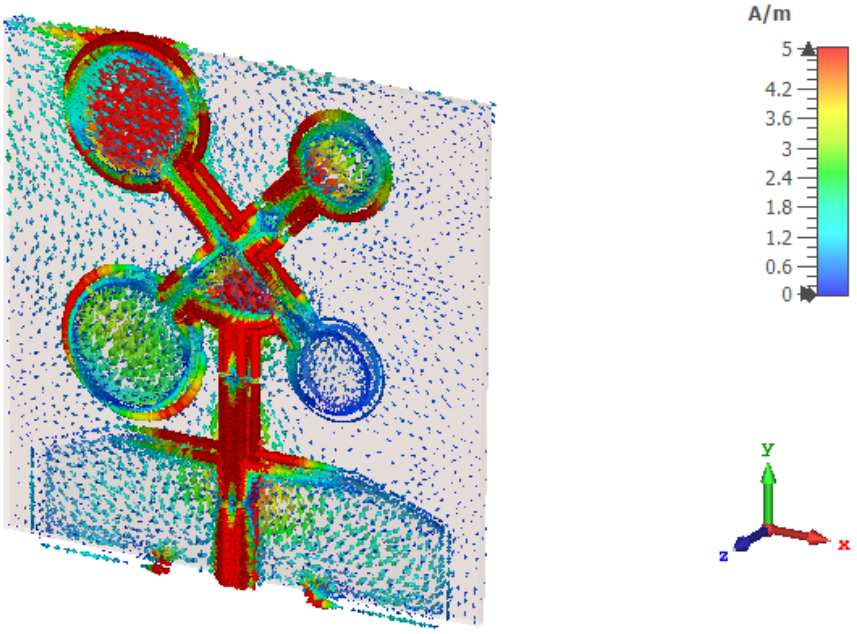

4. Conclusion

This project aimed the design and analysis of a dual band antenna for WBAN applications, operating at 3.5 GHz and 5.8 GHz. Experimenting an adapted geometry and using very common materials in the literature, the main antenna parameters were investigated and interpreted.

The proposed design achieved acceptable high gain and radiation efficiency levels at both resonant frequencies. But the analysis of real and imaginary parts of the impedance suggested that there was energy being wasted. When analyzing the surface current diagram, one of the possible interpretations is that the energy is not being properly distributed.

All these observations were very important for a good comprehension of the antenna operation and the emergence of ideas to improve the research, allowing the conclusion that the proposed antenna fits perfectly for WBAN applications, as the calculated parameters demonstrate this.

5. Future works

The analysis of the antenna parameters gave the basic knowledge to identify what needs to get better. The next step is to implement techniques that may improve the results and the analysis, such as beveling and others impedance matching techniques and more than one simulation environment for comparisons. Furthermore, the researchers intend to add SAR analysis, use human models simulations (Fig. 14) to ensure the absence of risk to health and, from then on, enable real measurements on people.

Figure 14. WBAN antenna simulation in human model in CST Studio [11].

In this work, direct design approach was adopted, in which the geometry of the antenna is constructed to obtain its frequency response. This study allowed a better understanding of the behavior of the antenna and the materials used. Based on this acquired knowledge, a research project is being developed that aims inverse design approach for construction and optimization of antennas using deep neural networks.

6. Referências

1. P. S. Hall and Y. Hao, Antennas and propagation for body-centric wireless communications. Boston, Mass: Artech House, 2012.

2. Yang,Deqiang., Hu,Jianzhong and L,Sihao. ,2018. A Low Profile UWB Antenna for WBAN Applications. IEEE Journals & Magazine. [online] Ieeexplore.ieee.org. Available at: <https://ieeexplore.ieee.org/document/8330748> [Accessed 30 Mar. 2019].

3. Singh, S., & Verma, S. (2021). Compact wideband circularly polarized bowtie slot antenna for WBAN applications. AEU-International Journal of Electronics and Communications, 136, 153777.

4. Kiani, S., Rezaei, P., & Fakhr, M. (2021). A CPW-fed wearable antenna at ISM band for biomedical

and WBAN applications. Wireless Networks, 27(1), 735-745.

5. A. Arif, M. Zubair, M. Ali, M. U. Khan and M. Q. Mehmood, "A Compact, Low-Profile Fractal Antenna for Wearable On-Body WBAN Applications," in IEEE Antennas and Wireless Propagation Letters, vol. 18, no. 5, pp. 981-985, May 2019, doi: 10.1109/LAWP.2019.2906829.

6. M. El Atrash, M. A. Abdalla and H. M. Elhennawy, "A Wearable Dual-Band Low Profile High Gain Low SAR Antenna AMC-Backed for WBAN Applications," in IEEE Transactions on Antennas and Propagation, vol. 67, no. 10, pp. 6378-6388, Oct. 2019, doi: 10.1109/TAP.2019.2923058.

7. Braham Chaouche, Youcef & Nedil, Mourad & Mabrouk, Ismail & Ramahi, Omar. (2022). A Wearable Circularly Polarized Antenna Backed by AMC Reflector for WBAN Communications. IEEE Access. 10. 10.1109/ACCESS.2022.3146386.

8. Dey, AB, Mitra, D, Arif, W. Design of CPW fed multiband antenna for wearable wireless body area network applications. Int J RF Microw Comput Aided Eng. 2020; 30:e22459. https://doi.org/10.1002/mmce.22459

9. Jawad, Mustafa Mohammed & Nik Abd Malik, Nik Noordini & Murad, Noor & Mohd Esa, Mona Riza & Ahmad, Mohd Riduan & Hussein, Yaqdhan. (2020). Design of substrate integrated waveguide with Minkowski-Sierpinski fractal antenna for WBAN applications. Bulletin of Electrical Engineering and Informatics. 9. 2455-2461. 10.11591/eei.v9i6.2194.

10. Mumin, Abdul & Alias, R. & Abdullah, Jiwa & Abdulhasan, Raed & Dahlan, S.H. & Joret, Ariffuddin. (2018). Performance Characteristics of Head-Worn Antenna based on Dielectric Substrate Over WBAN Application. International Journal of Engineering & Technology. 7. 403. 10.14419/ijet.v7i4.30.22345.

11. El Atrash, M., Abdalla, M., & Elhennawy, H. (2021). A fully-textile wideband AMC-backed antenna for wristband WiMAX and medical applications. International Journal of Microwave and Wireless Technologies, 13(6), 624-633. doi:10.1017/S1759078720001397

12. M. El Atrash, M. A. Abdalla and H. M. Elhennawy, "A Wearable Dual-Band Low Profile High Gain Low SAR Antenna AMC-Backed for WBAN Applications," in IEEE Transactions on Antennas and Propagation, vol. 67, no. 10, pp. 6378-6388, Oct. 2019, doi: 10.1109/TAP.2019.2923058.

13. C. Kissi et al., "Dual Band CPW-Fed Double Monopole Antenna for 2.4/5.8 GHz ISM band Medical Applications," 2019 International Symposium on Advanced Electrical and Communication Technologies (ISAECT), 2019, pp. 1-6, doi: 10.1109/ISAECT47714.2019.9069690.

14. Kaur, Amandeep & Malik, Praveen. (2021). Multiband Elliptical Patch Fractal and Defected Ground Structures Microstrip Patch Antenna for Wireless Applications. Progress In Electromagnetics Research B. 91. 157-173. 10.2528/PIERB20102704.

15. "CST Studio Suite Help," Mit.edu, 2022.

https://space.mit.edu/RADIO/CST_online/cst_studio_suite_help.htm (accessed Dec. 16, 2022).

16. C. Sun, Z. Wu e B. Bai, "A Novel Compact Wideband Patch Antenna," IEEE transactions on antennas and propagation, pp. 7334-7339, 12 2017 Dezembro.

17. Balanis, C. A. (2016). Antenna Theory: Analysis and Design. Reino Unido: Wiley.

18. Huang, Y. (2021). Antennas: From Theory to Practice. Reino Unido: Wiley.